Key Engineering Materials Vol. 605 (2014) pp 111-114

doi:10.4028/www.scientific.net/KEM.605.111

Coaxial Stub Resonator for Online Monitoring Early Stages of Corrosion

Natalia A. Hoog[1,3, a], Mateo J.J. Mayer[2,b], Henk Miedema[3,c],
Wouter Olthuis[1, d] and Albert van den Berg[1, e]

[1]BIOS - the Lab-on-a-Chip group, MESA+ Institute of Nanotechnology, University of Twente,
P.O. box 217, 7500 AE Enschede, The Netherlands,

[2]EasyMeasure B.V., Breestraat 22, 3811 BJ Amersfoort, The Netherlands,

[3]Wetsus, Agora 1, 8900 CC Leeuwarden, The Netherlands

[a]natalia.antonyuk@wetsus.nl, [b]info@easymeasure.nl,

[c]henk.miedema@wetsus.nl, [d]w.olthuis@utwente.nl, [e]a.vandenberg@utwente.nl

Keywords: Corrosion, Coaxial line, Stub Resonator.

Abstract. Here we demonstrate the proof-of-principle of a new type of flow-through sensor to assess the corrosion rate of metal surfaces. The method can be applied to all situations where metals are exposed to a corrosive (fluidic) environment, including, for instance, the interior of pipes and tubes. Our sensing device is based on the operating principle of a quarter wave length open-ended coaxial stub resonator. The method described here can be applied for on-line monitoring corrosion.

Introduction

The transmission line-based stub resonator flow-through sensor has been discussed in detail previously [1-4]. Here we specifically address the effect of corrosion of the surface of the inner conductor. In the absence of corrosion, both conductors are separated by a single dielectric, in this case a fluid. Oxidation of the metal surface of inner and/or outer conductor changes the electric properties of the sensor because it introduces a second (and possibly third) insulating layer between the two conductors with a permittivity that differs from that of the fluid. Corrosion changes the overall effective dielectric permittivity ε_{eff} and loss tangent $tg\delta_{eff}$ because it adds an extra dielectric layer in between inner and outer conductor (Fig. 1). Additionally, corrosion changes the surface texture which may result in conductor losses at high frequencies (skin effect). Given the dielectric constant and loss tangent of all layers are known, their overall effective values can be calculated according to Eqs. (1-5).

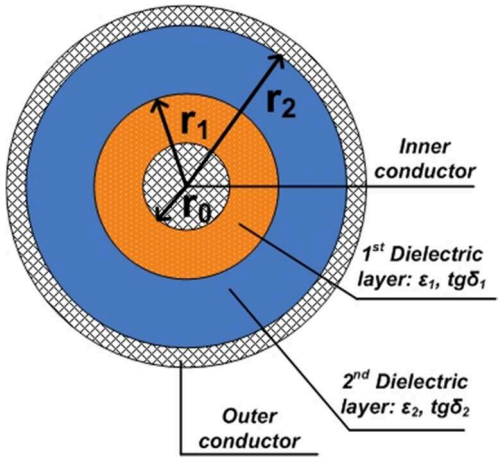

Fig 1. Schematic cross section of the coaxial stub resonator with two dielectric layers in between inner and outer conductor: corrosion layer (r_1, orange) and fluid (r_2, blue).

$$\varepsilon_{eff} = f(\varepsilon_1, \varepsilon_2, ..., \varepsilon_n) = C_{eff} / C_{vacuum} \quad (1)$$

$$C_{eff} = \left[\sum_{i=1}^{n} 1/C_i \right]^{-1} \quad (2)$$

$$C_n = \frac{2\pi\varepsilon_0\varepsilon_n}{\ln(r_n / r_{n-1})} \quad (3)$$

$$tg\delta_{eff} = \frac{C_1 tg\delta_2 + C_2 tg\delta_1}{C_1 + C_2} \quad (4)$$

$$f_{res} = (2n-1)/\left(2 \cdot \pi \cdot \sqrt{LC}\right) = c \cdot (2n-1)/(4 \cdot l \cdot \sqrt{\varepsilon_{eff}}) \quad (5)$$

where i represents the number of dielectric layers (-), L the distributed element inductance (H/m), ε_{eff}. the effective dielectric permittivity of a multi-layer dielectric, n the order number of resonance frequency and l the length of a resonator (m).

As a result of corrosion, the recorded amplitude-frequency (AF) plot shows a shift of the resonance frequency and/or a change of shape of the resonant peak(s), the latter reflecting changes in both skin effect and $tg\delta_{eff}$.

Results

Figure 2 shows the effect of corrosion of the inner conductor on recorded AF responses during a time period of 4 days for a flow-through sensor that was operated with tap water.

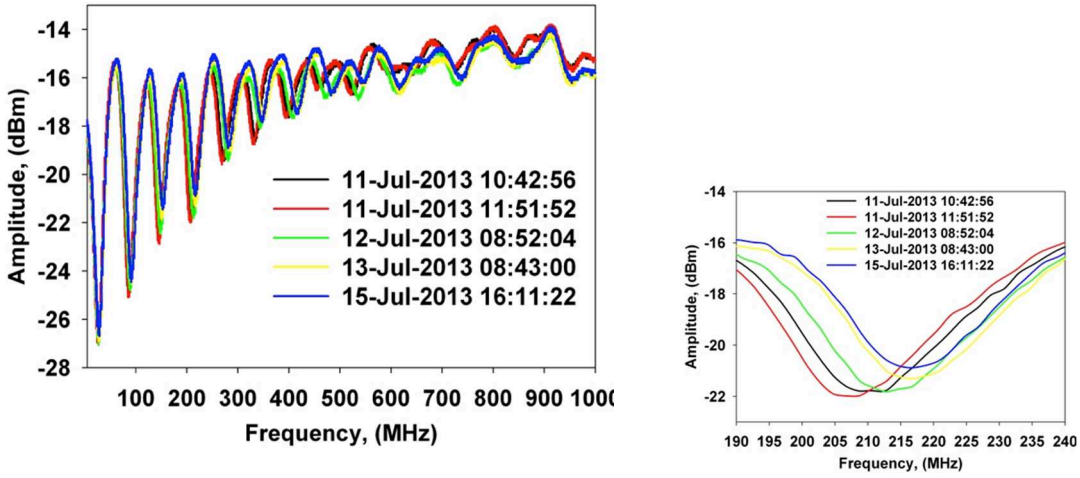

Fig. 2. Left: Recorded AF plots showing the effect of corrosion over a time period of 4 days (1000 points/scan). The right panels show the 1st (top) and 3th (bottom) resonance frequency peak of the left panel in more detail.

Figures 2 and 3 show that there is an observable effect in the AF response already after <24 hrs of operation, notably at higher frequencies. Similar data are shown in Fig. 4 but for a period of four days. Effects of corrosion are more pronounced at higher frequencies for two reasons. Firstly, according to Eq. 5 and given a certain change in ε_{eff}, the shift of f_{res} (Δf_{res}) is proportional to $c(2n-1)/4l$, implying a larger shift at higher n, i.e., at higher resonance frequencies. Secondly, as for the amplitude, e.g. the skin effect is more dominant at higher frequencies.

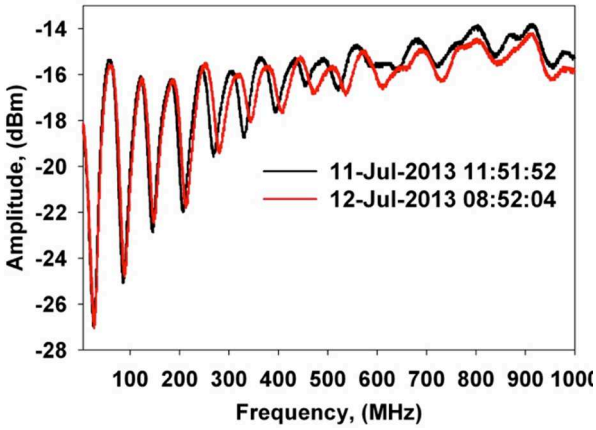

Fig. 3. Recorded AF plots showing the effect of corrosion over a period of ~2 days (1000 points/scan).

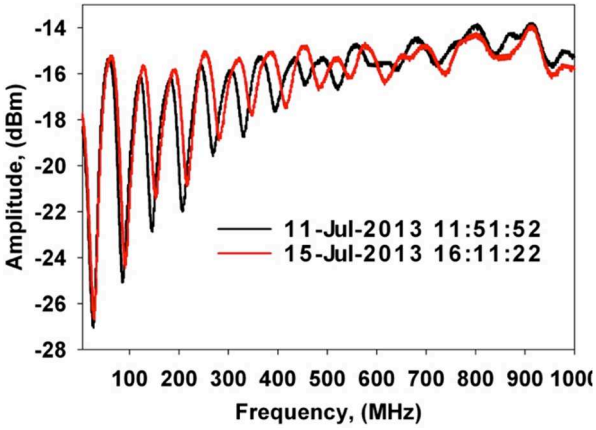

Fig. 4. Recorded AF plots showing the effect of corrosion over a period of ~2 days (1000 points/scan).

Calculated and measured f_{res} (of the 1st, 2nd, 3rd and 4th resonance frequencies) are compared in Table 1. The corrosion layer thickness of 20 µm is based on scanning electron microscopy (SEM) images at day 4. These SEM images showed an inhomogeneous corrosion layer on the inner conductor with a maximal thickness of 20 µm. The calculated shift in f_{res} of 1.5 MHz should therefore be considered the theoretical upper limit value. This may also explain the difference with the experimentally observed smaller shift of 0.7 MHz at 1st f_{res}.

Table 1 Comparison between calculated and measured f_{res} of the 1st resonance frequency, as well as ε_{eff} assuming either the absence or presence of a 20 µm homogenous corrosive layer covering the inner conductor. Measurements were performed with a 0.29 m flow-through quarter wavelength coaxial stub resonator, fed with tap water with conductivity σ 542 (µS/cm) and temperature t 20 °C as dielectric. Inner r_0 and outer r_2 conductor with diameters of 2.5 mm and 25.4 mm were made from steel and stainless 316L steel, respectively.

Corrosion Layer (µm)	ε_{eff}, (-)	Calculated 1st f_{res}, (MHz)	Measured 1st f_{res}, (MHz)	Calculated 2nd f_{res}, (MHz)	Measured 2nd f_{res}, (MHz)	Calculated 3rd f_{res}, (MHz)	Measured 3rd f_{res}, (MHz)	Calculated 4th f_{res}, (MHz)	Measured 4th f_{res}, (MHz)
0	79.0	28.1	27.3	84.3	86.2	140.6	145.7	196.9	206.7
20	70.9	29.7	28.0	92.2	91.3	153.6	153.6	215.0	217.2

One explanation for the differences between measured and calculated values of f_{res} is that the calculations do not account for the SMA connectors (total length 30 mm) used to connect transmission lines and resonator. Another reason might be that the steel used as inner conductor originally has a copper coating preventing oxidation. Careful removing this layer with sand paper prior to the experiments results in a characteristic surface roughness which in turn can have an effect on the skin effect and a minor effect on the inner conductor diameter. Especially during the first few hours of corrosion, the surface texture of the inner conductor will change at a fast rate, especially because of the initially large curvature of the imperfections on the inner conductor surface.

The experiments described here were performed using coaxial resonators with different geometrical parameters (length and diameter of inner and outer conductors), while operating in different frequency ranges. Besides steel and stainless steel 316L as inner conductor material, copper has been used. Despite all these differences, all type of experiments showed essentially very similar results.

Conclusions

The concept outlined here can be used for monitoring (early stages) of corrosion. Benefits of this technology over currently existing ones are: 1) the ease of corrosion assessment 2) the possibility of visual verification and replacement of the inner conductor and 3) the operational conditions spanning a wide range of frequencies. One challenge still is to distinguish effects due to corrosion from those caused by biofouling (i.e., adherence of bacterial plaque also affecting the AF response) and scaling (i.e., the deposition of salts). Once that hurdle has been successfully taken, the method outlined here offers an equipment-undemanding and cost-efficient tool for tracking the extent of corrosion as well as, for instance, testing the effectiveness of corrosion inhibitors. Currently performed research includes improving the sensitivity of the device by increasing the surface area of the inner conductor.

Acknowledgement

This work was performed in the TTIW-cooperation framework of Wetsus, Centre of Excellence for Sustainable Water Technology (www.wetsus.nl). Wetsus is funded by the Dutch Ministry of Economic Affairs, the European Union Regional Development Fund, the Province of Fryslân, the City of Leeuwarden and the EZ/Kompas program of “Samenwerkingsverband Noord-Nederland”. The authors thank the participants of the research theme “Sensoring” for the fruitful discussions and their financial support.

References

[1] N. A. Hoog-Antonyuk, W. Olthuis, M.J.J. Mayer, D. Yntema, H. Miedema, A. van den Berg, On-line fingerprinting of fluids using coaxial stub resonator technology, Sensors and Actuators B 163 (2012) 90-96, doi: dx.doi.org/10.1016/j.snb.2012.01.012.

[2] N.A. Hoog-Antonyuk, W. Olthuis, M.J.J. Mayer, H. Miedema, F.B.J. Leferink, A. van den Berg, Extensive Modeling of a Coaxial Stub Resonator for Online Fingerprinting of Fluids, Procedia Engineering (2012) pp. 310-313, doi: 10.1016/j.proeng.2012.09.145.

[3] M.J.J. Mayer, N. A. Hoog, RF antenna filter as a sensor for measuring a fluid, WO Patent 005084, 13 January 2011.

[4] N.A. Hoog, M.J.J. Mayer, Werkwijze en inrichting voor ingerprinting of het behandelen van een dielectricum in het algemeen en van water in het bijzonder, NL1038869, 16 August 2012.